

## THE HARMONIC FORCE FIELD AND ABSOLUTE INFRARED INTENSITIES OF DIACETYLENE

TH. KOOPS, T. VISSER and W. M. A. SMIT

*Analytical Chemistry Laboratory, University of Utrecht, Croesestraat 77A, 3522 AD Utrecht (The Netherlands)*

(Received 21 May 1984)

### ABSTRACT

The frequencies, harmonic force field and absolute IR intensities for  $C_4H_2$  and  $C_4D_2$  are reported. The experimental harmonized frequencies obey the Teller–Redlich product rule very well.

An approximate harmonic force field was obtained from a refinement procedure in which the starting values are adjusted in order to fit the experimental harmonized  $C_4H_2$  and  $C_4D_2$  frequencies. The starting force constant values were taken from the harmonic force field of propyne. The integrated IR intensities were determined according to the Wilson–Wells–Penner–Weber method, using nitrogen as a broadening gas at a pressure of 60 atm. The results of the  $F$ -sum rule clearly reveal the internal consistency of the measurements. Two sets of  $\partial\vec{\mu}/\partial S$  values can be derived from the experimental intensities by use of an iterative least-squares fitting procedure. One final set can be selected by applying the isotopic invariance criterion and by comparing with the corresponding derivatives of propyne. The final  $\partial\vec{\mu}/\partial S$  values are reduced to bond-charge parameters and atomic charges. The bond-charge parameter values are compared with the corresponding values of some common set of intensity parameters recently reported for the series  $C_2H_2$ ,  $CH_3CCH$  and  $CH_3CCCH_3$ .

### INTRODUCTION

In a previous study some common sets of bond charge parameters (bcp's) for acetylene, propyne and butyne-2 were presented [1]. In order to gain more insight into the applicability of the chosen parameter sets for the prediction of intensities of related molecules we have measured the absolute intensities of diacetylene.

Except for one band, the fundamental gas phase intensities were reported by Popov et al. in 1978 [2]. As far as we know, until now no intensities of deuterated derivatives have been reported. Since the measurements of Popov et al. were approximate (no pressure broadening) and incomplete, we decided to remeasure the  $C_4H_2$  intensities and also determine the intensities of  $C_4D_2$ . As usual, the obtained experimental intensity data were reduced to dipole moment derivatives with respect to symmetry coordinates (dmd's), which were further reduced to bcp's. A detailed comparison of these quantities

with the common sets mentioned above will shed some light on the limitations of the predictive abilities of such sets.

## EXPERIMENTAL

Diacetylene was prepared from 1,4-dichlorobutynes-2 and KOH by the method described in ref. 3, but on a much smaller scale. The diacetylene evolved was led away with  $N_2$  carrier gas, dried over  $CaCl_2$  and collected in a cold trap at  $-80^\circ C$ . The samples were purified twice by fractional distillation and stored at  $-35^\circ C$  in order to avoid decomposition. The only impurity detected in the IR spectra was a very small amount of propyne. The deuterated derivative was obtained by vigorously stirring  $C_4H_2$  in a solution of 1 N KOD in  $D_2O$  for two hours. After fractional distillation it appeared from MS as well as IR spectra that the purity of the samples was better than 92 mol%  $C_4D_2$ , the main impurity being  $C_4HD$ , while a very small amount of propyne was also detected.

## DETERMINATION OF THE HARMONIC FREQUENCIES

The IR gasphase spectra of  $C_4H_2$  and  $C_4D_2$  were recorded on Perkin-Elmer 180 and 580 B spectrophotometers (resolution better than  $1.1\text{ cm}^{-1}$  from  $4000\text{--}500\text{ cm}^{-1}$ , better than  $4.7\text{ cm}^{-1}$  from  $500\text{--}180\text{ cm}^{-1}$ ). The observed frequencies are given in Table 1 ( $d_0$ ) and Table 2 ( $d_2$ ). For comparison Table 1 also contains the frequencies reported by Jones [4] and Freund and Halford [5]. The overall agreement between the reported frequencies and the present values is quite good, the larger differences occurring for  $\nu_1 + \nu_8/\nu_4 + \nu_6$ ,  $\nu_4$ ,  $\nu_5 + 2\nu_6/\nu_5 + 2\nu_8$  and  $\nu_2 + \nu_9$ . However, the fundamental  $C_4H_2$  frequencies displayed in Table 3, indicate that our values for  $\nu_5 + 2\nu_6/\nu_5 + 2\nu_8$  and  $\nu_2 + \nu_9$  should be preferred. The present  $\nu_8$  value is in nice agreement with the one reported by Hardwick et al. [6], who obtained his value from a rotational analysis of this band. Our  $\nu_9$  frequency is in complete agreement with the value observed by Winther [7]. The fundamental frequencies of the Raman active modes were, if possible, determined from difference bands observed in the IR gas-phase spectra. In this way the frequencies of the  $\nu_1$ ,  $\nu_2$  and  $\nu_6$  modes of  $C_4H_2$  were obtained. The frequency of  $\nu_1$  was obtained both from  $\nu_1 - \nu_9$  and  $\nu_1 - \nu_8$ . The possible Fermi resonance of  $\nu_1 - \nu_9$  with  $\nu_2 + \nu_8$  on the one hand and of  $\nu_1 - \nu_8$  with  $\nu_2 + \nu_8$  and  $\nu_5 + \nu_6$  on the other hand seems to be absent in view of the nearly identical  $\nu_1$  values obtained from the two difference bands ( $\nu_1 - \nu_9$  gives  $\nu_1 = 3331\text{ cm}^{-1}$ , whereas  $\nu_1 - \nu_8$  yields  $\nu_1 = 3333\text{ cm}^{-1}$ ). The average value is given in Table 3.

The frequencies of  $\nu_2$  and  $\nu_6$ , deduced from  $\nu_2 - \nu_9$  and  $\nu_4 - \nu_6$  respectively, are in nice agreement with the gas-phase values reported by Jones [4]. The frequencies of the two remaining Raman active modes, i.e.  $\nu_3$  and  $\nu_7$ , were taken from Jones [4]. Winther [7] reported the frequency of  $\nu_7 - \nu_9$  to be at  $262\text{ cm}^{-1}$ , leading to a value of  $482\text{ cm}^{-1}$  for  $\nu_7$ , which is in complete

TABLE 1

Observed IR gas-phase frequencies ( $\text{cm}^{-1}$ ) for  $\text{C}_4\text{H}_2$  <sup>a</sup>

This work	Jones <sup>b</sup>	F & H <sup>c</sup>	Assignment <sup>d</sup>
3940 s	3948 s	3939	$\nu_1 + \nu_8; \nu_4 + \nu_6(\Pi_u)?$
3550 ms	3547 m	3554	$\nu_1 + \nu_9(\Pi_u)$
3332 vs	3329 vs	3324	$\nu_4(\Sigma_u^+)$
3252 ms	3247 s	3246	$\nu_5 + 2\nu_6; \nu_5 + 2\nu_8(\Sigma_u^+ + \Delta_u)$
3111 m	3109 m	3109	$\nu_1 - \nu_9(\Pi_u)$
2980			propyne
2910			propyne
2810 vw	2805 w	2805	$\nu_2 + \nu_8(\Pi_u)$
2705 m	2705 m	2704	$\nu_1 - \nu_8; \nu_4 - \nu_6(\Pi_u)$
2642 w	2642 w	2642	$\nu_3 + \nu_6(\Pi_u)$
2499 w	2496 w	2495	$\nu_3 + \nu_7(\Pi_u)$
2405 w	2401 w	2399	$\nu_2 + \nu_9(\Pi_u)$
2142			propyne
2020 s	2020 s	2018	$\nu_3(\Sigma_u^+)$
1966 vw	1964 w	n.o.	$\nu_2 - \nu_9(\Pi_u)$
1865 w	1864 w	1862	$2\nu_6 + \nu_8; 3\nu_8(\Pi_u + \phi_u)$
1462 m	1465 w	1463	$2\nu_6 + \nu_9(\Pi_u + \phi_u)$
1450			propyne
1390			propyne
1242 vs	1241 vs	1240	$\nu_6 + \nu_8(\Sigma_u^+ + \Sigma_u^- + \Delta_u)$
1112 m	1113 m	1112	$\nu_1 + \nu_8(\Sigma_u^+ - \Sigma_u^- + \Delta_u)$
1020 m	1020 w	n.o.	$2\nu_6 - \nu_9; 2\nu_8 - \nu_9(\Pi_u - \phi_u)$
844 m	846 m	845	$\nu_6 + \nu_9(\Sigma_u^+ + \Sigma_u^- + \Delta_u)$
700 s	701 s	701	$\nu_7 + \nu_9(\Sigma_u^+ + \Sigma_u^- + \Delta_u)$
639			propyne
628 vs	630 vs	630	$\nu_6(\Pi_u)$
220 s	n.m.	n.m.	$\nu_9(\Pi_u)$

<sup>a</sup>w = weak, m = medium, s = strong, v = very, n.o. = not observed, n.m. = not measured.<sup>b</sup>Ref. 4. <sup>c</sup>Ref. 5. <sup>d</sup>Apart from a few exceptions only fundamentals and binary combinations have been considered.

agreement with the gas-phase value of ref. 4. Our  $2\nu_6 - \nu_9$  frequency value leads to a  $2\nu_6$  value of  $1240 \text{ cm}^{-1}$ . Using this value and the frequency of  $\nu_6$  both the anharmonicity constant and harmonic frequency for this mode may be calculated, yielding  $x_6 = 0.024$  and  $\omega_6 = 644 \text{ cm}^{-1}$ , whereas the  $\nu_6$  and  $2\nu_6$  values of  $\text{C}_4\text{HD}$  (see Table 2) give  $x_6 = 0.022$  and  $\omega_6 = 642 \text{ cm}^{-1}$ . The average values have been used in this work.

The anharmonicity constant, obtained in this way, is in reasonable agreement with the one reported by Duncan et al. [8],  $x_6 = 0.02$ , lending confidence in the use of the anharmonicity constants reported by the same authors for the remaining modes of diacetylene. From the gas-phase IR spectra of  $\text{C}_4\text{D}_2$  the frequencies of the following Raman active modes were derived:  $\nu_1$  from  $\nu_1 - \nu_9$  and  $\nu_1 - \nu_8$ ,  $\nu_2$  from  $\nu_2 - \nu_9$ ,  $\nu_7$  from  $\nu_4 - \nu_7$  and  $\nu_6$  from  $\nu_4 - \nu_6$ .

The  $\nu_1$  values obtained from  $\nu_1 - \nu_9$  and  $\nu_1 - \nu_8$  are in good agreement, indicating that these difference bands are not involved in Fermi resonance

TABLE 2

Observed IR gas-phase frequencies ( $\text{cm}^{-1}$ ) for  $\text{C}_4\text{D}_2$  <sup>a</sup>

Frequency	Assignment <sup>b</sup>	Frequency	Assignment <sup>b</sup>
3938 w	$\nu_1 + \nu_6(\text{C}_2\text{HD})?$	2068 vw	$\nu_1 - 2\nu_6(\text{C}_2\text{HD})?$
3604 vw	$2\nu_6 + \nu_4(\Sigma_u^+ + \Delta_u + \Gamma_u)$	1892 m	$\nu_3(\Sigma_u^+)$
3535 vw	$\nu_1 + \nu_9(\text{C}_2\text{HD})$	1866 w	$\nu_2 - \nu_9(\Pi_u)$
3438 w	$\nu_3 + \nu_4(\Sigma_u^+)$	1450	propyne
3332 m	$\nu_1(\text{C}_2\text{HD})$	1390	propyne
3084 m	$\nu_4 + \nu_6(\Pi_u)$	1242 m	$2\nu_6(\text{C}_2\text{HD})$
3054 m	$\nu_4 + \nu_7(\Pi_u)$	1162 w	$\nu_6 + \nu_7 + \nu_9(\Pi_u + \phi_u)$
2980	propyne	996 s	$\nu_6 + \nu_8(\Sigma_u^+ + \Sigma_u^- + \Delta_u)$
2910	propyne	951 s	$\nu_7 + \nu_8(\Sigma_u^+ + \Sigma_u^- + \Delta_u)$
2806 w	$\nu_1 + \nu_9(\Pi_u)$	853 m	$\nu_3(\text{C}_2\text{HD})?$
2734 m	$\nu_3 + \nu_5(\Sigma_u^+)$	758 vw	$\nu_6 + \nu_7 - \nu_9(\Pi_u + \phi_u)$
2598 vs	$\nu_4(\Sigma_u^+)$	700 s	$\nu_6 + \nu_8(\Sigma_u^+ + \Sigma_u^- + \Delta_u)$
2404 w	$\nu_1 - \nu_9(\Pi_u)$	667 w	$\nu_7 + \nu_9(\Sigma_u^+ + \Sigma_u^- + \Delta_u)$
2388 w	$\nu_5 + \nu_6(\Pi_u)$	639	propyne
2360 m	$\nu_5 + \nu_7(\Pi_u)$	628 s	$\nu_6(\text{C}_2\text{HD})$
2268 m	$\nu_2 + \nu_9(\Pi_u)$	497 vs	$\nu_8(\Pi_u)$
2138 w	$\nu_4 - \nu_7(\Pi_u)$	464 m	$\nu_7(\text{C}_2\text{HD})$
2108 w	$\nu_1 - \nu_8(\Pi_u)$	202 s	$\nu_9(\Pi_u)$
2098 vw	$\nu_4 - \nu_6(\Pi_u)$		

<sup>a</sup>v = very, w = weak, m = medium, s = strong. <sup>b</sup>Apart from a few exceptions only fundamentals and binary combinations have been considered.

TABLE 3

Observed fundamental gas-phase frequencies ( $\text{cm}^{-1}$ ) for  $\text{C}_4\text{H}_2$  and  $\text{C}_4\text{D}_2$ 

		$\text{C}_4\text{H}_2$		$\text{C}_4\text{D}_2$
		This work	Jones [4]	
$\Sigma_g^+$	$\nu_1$	3332	3329	2606
	$\nu_2$	2186	2184	2068
	$\nu_3$	874 <sup>a</sup>	874	846
$\Sigma_u^+$	$\nu_4$	3333	3329	2598
	$\nu_5$	2020	2020	1892
$\Pi_u$	$\nu_6$	628	627	500
	$\nu_7$	482 <sup>a</sup>	482	460
$\Pi_u$	$\nu_8$	628	630	497
	$\nu_9$	220	n.o.	202

<sup>a</sup>Taken from ref. 4

with nearby combination bands of the same symmetry (see Table 2). The rather isolated position of the  $\nu_2 - \nu_9$  difference bands makes it free of Fermi resonance, thus yielding an unperturbed  $\nu_2$  value. Since Fermi resonance between  $\nu_4 - \nu_7$  and  $\nu_4 - \nu_6$  cannot be excluded the values of the fundamental frequencies derived thereof may be somewhat less reliable. The  $\nu_3$

frequency of  $C_4D_2$  was taken from the Raman spectrum of a  $CCl_4$  solution of this compound, assuming the difference between the gas-phase and solution value to be zero, in accordance with the result found for the corresponding frequency of  $C_4H_2$ . The gas-phase frequencies of  $C_4D_2$  determined as described above are collected in Table 3.

#### DETERMINATION OF AN APPROXIMATE HARMONIC FORCE FIELD

Using the above calculated anharmonicity factor for the hydrogen bending modes  $\nu_6$  and  $\nu_8$  and the approximate anharmonicity factors of Duncan et al. [8] for the remaining modes, the harmonized frequencies of  $C_4H_2$  and  $C_4D_2$ , as shown in Table 4, were obtained. In the case of  $C_4D_2$  Dennison's rule [9] was used in order to adjust the anharmonicity constants.

Application of the Teller—Redlich product rule [10] shows a very satisfactory internal consistency, as can be seen from Table 5. The calculated harmonic frequencies, also listed in Table 4, were obtained from the final force constants given in Table 6. The starting values, listed in the same Table, were obtained from the harmonized force field of propyne, as reported by Duncan et al. [8]. As a first step the force field of propyne on a symmetry coordinate basis was converted to an internal coordinate basis. In the next step the appropriate force constants were transferred to the diacetylene molecule and converted to the symmetry coordinates summarized in Table 7. The adopted geometry parameters [11] for diacetylene are also included in Table 7. The internal coordinates are defined in Fig. 1.

Taking into account the delocalization of the  $\pi$  electrons across the  $C\equiv C$  and  $C-C$  bonds the interaction constant  $f_{r_1r_3}$ , which describes the interaction between these bonds, may be expected to have a larger value in diacetylene than in propyne.

TABLE 4

Experimental and calculated harmonic frequencies ( $cm^{-1}$ ) for  $C_4H_2$  and  $C_4D_2$

	$C_4H_2$		$C_4D_2$ <sup>a</sup>	
	Exp.	Calc.	Exp.	Calc.
$\omega_1$	3489	3492	2701	2701
$\omega_2$	2219	2220	2098	2097
$\omega_3$	887	887	859	859
$\omega_4$	3490	3492	2693	2689
$\omega_5$	2051	2049	1919	1920
$\omega_6$	643	639	509	514
$\omega_7$	489	488	467	461
$\omega_8$	643	648	506	507
$\omega_9$	223	223	205	206

<sup>a</sup>In the case of  $C_4D_2$ , Dennison's rule [13] was used in order to adjust the anharmonicity constants.

TABLE 5

Teller—Redlich product rule results for  $C_4H_2$  and  $C_4D_2$ 

Product rule expression	Exp.	Theoretical
$\frac{(\omega_1\omega_2\omega_3)_D}{(\omega_1\omega_2\omega_3)_H} = \left(\frac{m_H}{m_D}\right)^{1/2}$	0.7088	0.7074
$\frac{(\omega_4\omega_7)_D}{(\omega_4\omega_5)_H} = \left(\frac{m_H}{m_D}\right)^{1/2} \left(\frac{M_D}{M_H}\right)^{1/2}$	0.7220	0.7215
$\frac{(\omega_4\omega_7)_D}{(\omega_6\omega_7)_H} = \left(\frac{m_H}{m_D}\right)^{1/2} \left(\frac{I_{xH}}{I_{xD}}\right)^{1/2}$	0.7560	0.7602
$\frac{(\omega_4\omega_9)_D}{(\omega_8\omega_9)_H} = \left(\frac{m_H}{m_D}\right)^{1/2} \left(\frac{M_D}{M_H}\right)^{1/2}$	0.7234	0.7215

TABLE 6

Harmonic force constants (m dyn A<sup>-1</sup>) for diacetylene

Force constant	Starting	Final	S and P <sup>a</sup>
$f_{r_1r_1} = f_{r_3r_3}$	6.513	6.515	5.92
$f_{r_1r_2} = f_{r_3r_4}$	-0.092	-0.097	0.00
$f_{r_1r_3} = f_{r_3r_3}$	0.075	0.073	0.00
$f_{r_2r_2} = f_{r_4r_4}$	15.95	15.55	14.98
$f_{r_2r_3} = f_{r_4r_3}$	0.4-0.8 <sup>b</sup>	0.58	0.55
$f_{r_2r_4} = f_{r_4r_2}$	0.00 <sup>b</sup>	-0.29	-0.38
$f_{r_3r_3}$	5.504	7.12	6.99
$f_{\phi_{1x}\phi_{1x}} = f_{\phi_{2x}\phi_{2x}}$	0.235	0.241	0.218
$f_{\phi_{1x}\phi_{2x}} = f_{\phi_{2x}\phi_{1x}}$	0.00	0.00	0.00
$f_{\phi_{1x}\beta_{1x}} = f_{\phi_{2x}\beta_{2x}}$	0.108	0.108	0.1035
$f_{\phi_{1x}\beta_{2x}} = f_{\phi_{2x}\beta_{1x}}$	0.00	0.00	0.00
$f_{\beta_{1x}\beta_{1x}} = f_{\beta_{2x}\beta_{2x}}$	0.369	0.351	0.341
$f_{\beta_{1x}\beta_{2x}} = f_{\beta_{2x}\beta_{1x}}$	0.00	0.008	0.012

<sup>a</sup>Sipos and Phibbs [12]. <sup>b</sup>Varied between the given limits. The pertaining optimum value for  $f_{r_2r_4}$  depends heavily on the value chosen for  $f_{r_2r_3}$  (see text).

A whole family of force field solutions with different values for  $f_{r_2r_3}$  can be obtained, which all equally well predict the  $C_4H_2$  frequencies. We derived a number of different force fields by choosing a preset value for  $F_{23} = 2^{1/2}f_{r_2r_3}$  and fitting the diagonal symmetry force constants to the experimental harmonized  $C_4H_2$  frequencies. At this point it may be noted that adjustment of the diagonal symmetry force constants  $F_{22}$ ,  $F_{55}$ ,  $F_{77}$  and  $F_{99}$  implies refinement of the non-diagonal elements  $f_{r_2r_4}$  and  $f_{\beta_{1x}\beta_{2x}}$  on an internal coordinate basis (see Table 7).

TABLE 7

Symmetry coordinates, force constant relations and geometry parameters for diacetylene

Symmetry coordinates	Force constant relations	
$S_1 = 2^{-1/2}(\Delta r_1 + \Delta r_5)$	$F_{11} = f_{r_1 r_1} + f_{r_1 r_5}$	$F_{12} = f_{r_1 r_2} + f_{r_1 r_4}$
$S_2 = 2^{-1/2}(\Delta r_2 + \Delta r_4)$	$F_{22} = f_{r_2 r_2} + f_{r_2 r_4}$	$F_{13} = 2^{1/2} f_{r_1 r_3}$
$S_3 = \Delta r_3$	$F_{33} = f_{r_3 r_3}$	$F_{23} = 2^{1/2} f_{r_2 r_3}$
$S_4 = 2^{-1/2}(\Delta r_1 - \Delta r_5)$	$F_{44} = f_{r_1 r_1} - f_{r_1 r_5}$	$F_{45} = f_{r_1 r_2} - f_{r_1 r_4}$
$S_5 = 2^{-1/2}(\Delta r_2 - \Delta r_4)$	$F_{55} = f_{r_2 r_2} - f_{r_2 r_4}$	$F_{67} = f_{\phi_{1x} \beta_{1x}} - f_{\beta_{1x} \phi_{2x}}$
$S_{6x} = 2^{-1/2}(\Delta \phi_{1x} - \Delta \phi_{2x})A$	$F_{66} = f_{\phi_{1x} \phi_{1x}} - f_{\phi_{1x} \phi_{2x}}$	$F_{89} = f_{\phi_{1x} \beta_{2x}} + f_{\beta_{1x} \phi_{2x}}$
$S_{7x} = 2^{-1/2}(\Delta \beta_{1x} - \Delta \beta_{2x})A$	$F_{77} = f_{\beta_{1x} \beta_{1x}} - f_{\beta_{1x} \beta_{2x}}$	
$S_{8x} = 2^{-1/2}(\Delta \phi_{1x} + \Delta \phi_{2x})A$	$F_{88} = f_{\phi_{1x} \phi_{1x}} + f_{\phi_{1x} \phi_{2x}}$	
$S_{9x} = 2^{-1/2}(\Delta \beta_{1x} + \Delta \beta_{2x})A$	$F_{99} = f_{\beta_{1x} \beta_{1x}} + f_{\beta_{1x} \beta_{2x}}$	
Geometry parameters <sup>b</sup>		
$r_{C-H} = 1.093 \text{ \AA}$ $r_{C \equiv C} = 1.217 \text{ \AA}$ $r_{C-C} = 1.383 \text{ \AA}$		

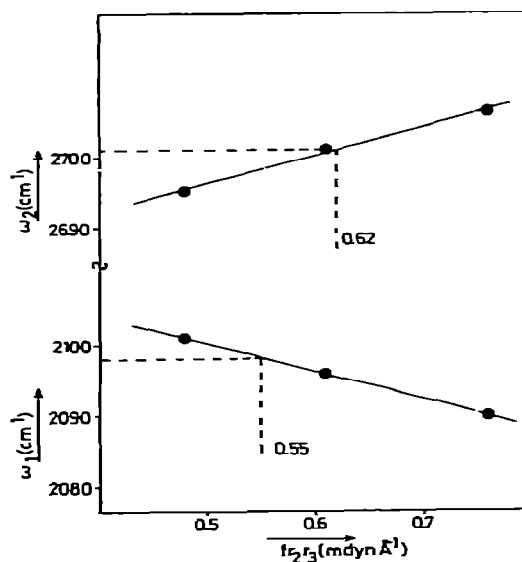
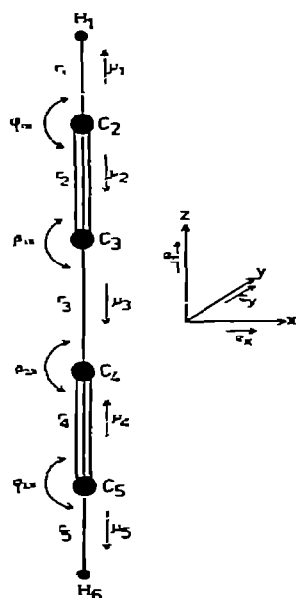
<sup>a</sup> $F_{ij} = F_{ji}$ , only expressions for non-zero force constants are given. <sup>b</sup>Ref. 11.

Fig. 1. Definition of internal coordinates, bond moment directions, Cartesian axis system and unit vectors.

Fig. 2 Calculated ω<sub>1</sub> and ω<sub>2</sub> frequency values for C<sub>4</sub>D<sub>2</sub> as a function of the interaction force constant f<sub>2r3</sub>.

Prediction of the corresponding  $C_4D_2$  frequencies with these force fields showed that, in particular,  $\omega_1$  and  $\omega_2$  of the deuterated derivative are sensitive to the value of  $f_{r_2r_3}$ , the dependence being depicted in Fig. 2. It appears from Fig. 2 that  $\omega_1$  leads to  $f_{r_2r_3} = 0.62$  mdyn  $\text{\AA}^{-1}$ , whereas  $\omega_2$  yields  $f_{r_2r_3} = 0.55$  mdyn  $\text{\AA}^{-1}$ . The average value has been adopted in the present calculations. The interaction force constants  $f_{r_1r_2}$ ,  $f_{\beta_{1x}\phi_{1x}}$ ,  $f_{\beta_{2x}\phi_{1x}}$  and  $f_{\phi_{1x}\phi_{2x}}$  have been constrained to zero, leading to  $F_{11} = F_{44}$ ,  $F_{66} = F_{88}$  and  $F_{67} = F_{76} = F_{89} = F_{98}$  as becomes apparent from the relations between the force constants on symmetry and internal coordinate basis given in Table 7. The final force constant values, displayed in Table 6, were obtained from the starting set by a refinement procedure. First, the diagonal symmetry force constants were fitted to the experimental harmonized frequencies of  $C_4H_2$  and  $C_4D_2$ . Next, the two interaction force constants  $f_{r_1r_2}$  and  $f_{r_1r_3}$  were adjusted, keeping the remaining force constants fixed. The final force constant values are given in Table 6 on an internal coordinate basis since this facilitates the following discussion. The symmetry force constant values are easily obtained from the relations given in Table 7. In the refinement procedure a somewhat lower weight was assigned to the experimental  $\omega_6$  and  $\omega_7$  values of the deuterated derivative, due to the possible Fermi resonance between the difference bands  $\nu_4 - \nu_6$  and  $\nu_4 - \nu_7$ . The influence of the  $\pi$  electron delocalization on the C—C and C $\equiv$ C stretching force constants is clearly demonstrated by the rather large difference between the starting and final values. The  $f_{r_3r_4}$  force constant changes from 5.504 to 7.12 mdyn  $\text{\AA}^{-1}$  in going from propyne to diacetylene while the  $f_{r_2r_3}$  value decreases from 15.95 to 15.55 mdyn  $\text{\AA}^{-1}$ . The small value found for  $f_{\beta_{1x}\beta_{2x}}$  justifies that zero values were assigned to  $f_{\beta_{1x}\phi_{2x}}$ ,  $f_{\beta_{2x}\phi_{1x}}$  and  $f_{\phi_{1x}\phi_{2x}}$ . For comparison the anharmonic force field of Sipos and Phibbs [12] is also summarized in Table 6. Since this force field is based on experimental frequencies, no detailed comparison with the present results will be made. The diagonal force constant values, show the same pattern, while obviously, the harmonic values are somewhat larger than the corresponding anharmonic values. Further, it may be noted that the values for the interaction force constants  $f_{r_1r_3}$ ,  $f_{r_2r_4}$  and  $f_{\beta_{1x}\beta_{2x}}$  as given by Sipos and Phibbs [12] are quite comparable to our values. This is, however, not very surprising, since they used almost the same method to fix the values of the interaction constants.

The overall agreement between the experimental and calculated harmonic frequencies is very satisfactory; the larger discrepancies occur for  $\omega_6$ ,  $\omega_8(d_0)$  and  $\omega_4$ ,  $\omega_6$ ,  $\omega_7(d_2)$ . However, taking into account that the experimental values for  $\omega_6(d_2)$  and  $\omega_7(d_2)$  may suffer from Fermi resonance as mentioned above, the agreement for these may in fact be very good.

#### MEASUREMENT OF THE INTEGRATED INTENSITIES

The intensity measurements were made on a Perkin-Elmer model 180 spectrophotometer equipped with a Data Control interface and a digital magnetic recorder (PE 109).



Interference from atmospheric water and carbon dioxide was prevented by flushing with dry and  $\text{CO}_2$ -free air. A stainless steel absorption cell with KRS-5 windows and an effective pathlength of 5.15 cm was used for the measurement of all fundamentals with the exception of  $\nu_9$ . The  $\nu_9$  intensities were measured in a stainless steel absorption cell with Si windows and an effective pathlength of 15.21 cm.

Sample pressures ranged from 0.0–35.0 cm Hg for  $\text{C}_4\text{H}_2$  and from 0.0–53.5 cm Hg for  $\text{C}_4\text{D}_2$ . Sample pressures lower than 2.5 cm Hg were obtained from carefully premixed samples of diacetylene in nitrogen. Due to polymerization of diacetylene only diluted samples which were freshly prepared could be used. All samples were pressurized by adding 60 atm. of very pure nitrogen, with the exception of the samples measured in the Si-cell, which allows a broadening pressure of only 1 atm. The integrated intensities were determined according to the Wilson–Wells–Penner–Weber–method [13, 14]. The spectra were sampled with an interval of  $1\text{ cm}^{-1}$  and numerically integrated. At 60 atm. pressure and the applied spectral slit width (resolution better than  $1.1\text{ cm}^{-1}$ ) the vibration–rotation lines were sufficiently broadened to give linear Beer's law plots, as shown in Figs. 3–5.

The slopes of the Beer's law plots, corresponding to the integrated intensities, were obtained from a linear least-squares analysis of the intensity data. In the error calculation both the random errors in band areas and sample pressures were taken into account [15]. Apart from the  $\nu_9(d_0)$  intensity, the errors stated for the absolute intensities are the standard deviations, which

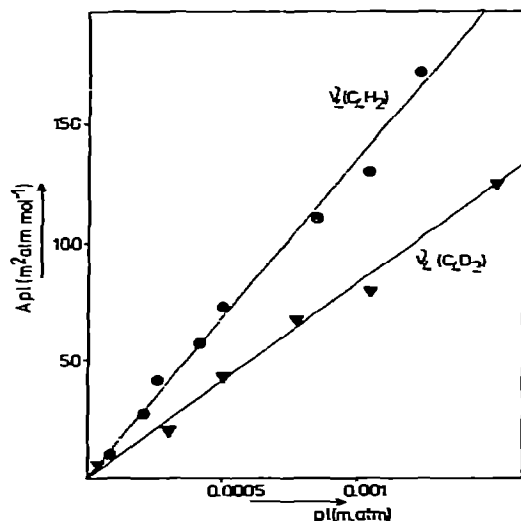


Fig. 3. Beer's law plots for the  $\nu_4$  fundamentals of  $\text{C}_4\text{H}_2$  and  $\text{C}_4\text{D}_2$ .

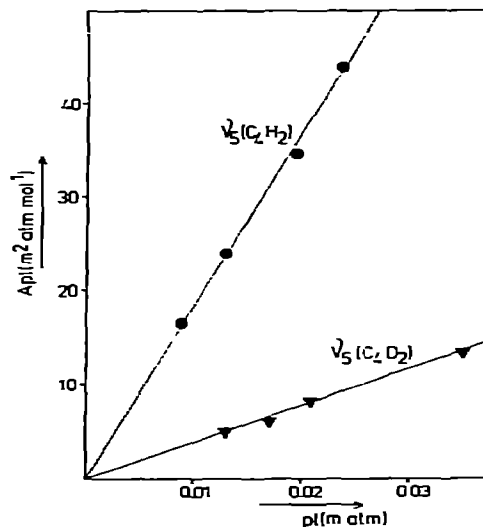


Fig. 4. Beer's law plots for the  $\nu_5$  fundamentals of  $\text{C}_4\text{H}_2$  and  $\text{C}_4\text{D}_2$ .

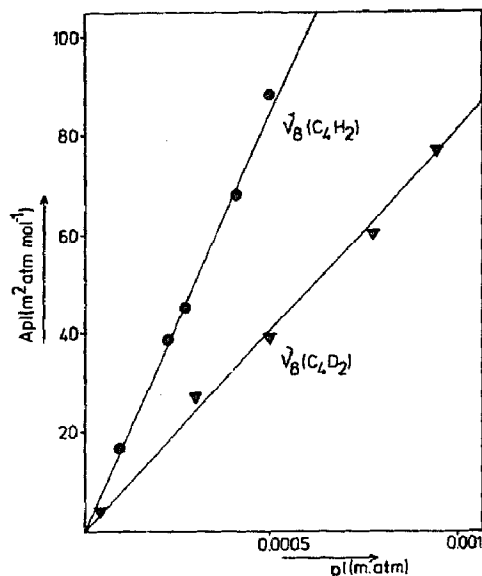


Fig. 5. Beer's law plots for the  $\nu_8$  fundamentals of  $C_4H_2$  and  $C_4D_2$ .

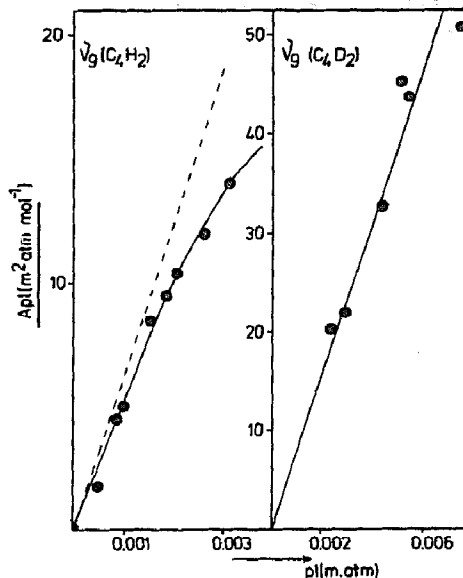


Fig. 6. Beer's law plots for the  $\nu_9$  fundamentals of  $C_4H_2$  and  $C_4D_2$ .

resulted from the least-squares analysis. The measurements of the  $\nu_9$  fundamentals were performed with a resolution of  $4.1 \text{ cm}^{-1}$  or better and a pressure broadening of only 1 atm. As shown in Fig. 6, the Beer's law plot for  $\nu_9(d_0)$  apparently deviates from linearity, in contrast with the same plot for  $C_4D_2$ . This behaviour was also found for the corresponding modes of butyne-2 ( $d_0$ ) and butyne-2 ( $d_6$ ) [16]. The absolute intensity of the  $\nu_9(d_0)$  band was obtained from a least-squares fitting of a cubic spline function through the data points. The derivative at zero sample pressure was taken as the absolute intensity. An estimated error of 5% was assigned to this value.

The following integration intervals were used for  $C_4H_2$ :  $\nu_4$ :  $3500\text{--}3150 \text{ cm}^{-1}$ ;  $\nu_5$ :  $2060\text{--}1950 \text{ cm}^{-1}$ ;  $\nu_8$ :  $680\text{--}535 \text{ cm}^{-1}$ ;  $\nu_9$ :  $245\text{--}205 \text{ cm}^{-1}$  and for  $C_4D_2$ :  $\nu_4$ :  $2750\text{--}2150 \text{ cm}^{-1}$ ;  $\nu_5$ :  $2050\text{--}1830 \text{ cm}^{-1}$ ;  $\nu_8$ :  $560\text{--}420 \text{ cm}^{-1}$  and  $\nu_9$ :  $245\text{--}182 \text{ cm}^{-1}$ .

No pressure, nor intensity corrections were made for the small amounts of propyne present in the diacetylene samples, since in all cases the resulting corrections were estimated to be smaller than the random errors in the experimental intensities. The same holds for the  $C_4D_2$  measurements. However, it was necessary to make intensity and pressure corrections for the  $C_4HD$  impurity present in the  $C_4D_2$  samples. The amount of  $C_4HD$  was determined as following. During the measurements of the  $C_4D_2$  fundamentals in the  $3000\text{--}400 \text{ cm}^{-1}$  region, the band area of the C—H stretching mode of  $C_4HD$  at  $3332 \text{ cm}^{-1}$  was also determined. From the measured band area of this

mode and the predicted absolute intensity value for this mode based on the  $C_4H_2$  intensities (see last column of Table 12) the amount of  $C_4HD$  was calculated. All  $C_4D_2$  pressure and intensity measurements were accordingly adjusted. Corrections for  $\nu_9(d_2)$  were made by using the average  $C_4HD$  concentration derived from the above-mentioned measurements. The absolute intensities obtained in this way are displayed in Table 8 the  $C_4H_2$  intensities reported by Popov et al. [2] are given for comparison.

The difference between our values and those reported by Popov et al. [2] may partly be ascribed to the rather poor experimental conditions of the older measurements (no pressure broadening). However, the reason for the large discrepancy between the  $A_4$  intensities is not clear. The internal consistency of the measurements was checked by applying the  $F$ -sum rule [17]. The results, collected in Table 9, reveal a very satisfactory consistency for the present  $\Sigma_u$  type intensities, showing that the  $A_4$  value reported by Popov et al. is clearly at fault. The agreement between the  $\Pi_u$  type intensities is somewhat less, although the differences are not significant taking into account the error limits.

TABLE 8

Experimental intensities ( $\text{km mol}^{-1}$ ) for  $C_4H_2$  and  $C_4D_2$

Compound	$\nu_i$ ( $\text{cm}^{-1}$ )	$A_i$	
		This work	Popov et al. <sup>a</sup>
$C_4H_2$	$\nu_4$ 3333	$136 \pm 6$	$67 \pm 3$
	$\nu_5$ 2020	$1.84 \pm 0.09$	$1.50 \pm 0.08$
	$\nu_8$ 628	$172 \pm 12$	$185 \pm 9$
	$\nu_9$ 220	$6.2 \pm 0.3$	— <sup>b</sup>
$C_4D_2$	$\nu_4$ 2598	$84 \pm 4$	
	$\nu_5$ 1892	$0.39 \pm 0.05$	
	$\nu_8$ 497	$80 \pm 5$	
	$\nu_9$ 202	$8.1 \pm 1.4$	

<sup>a</sup>Ref 2 <sup>b</sup>Not measured

TABLE 9

$F$ -sum rule results ( $\text{cm}^3 \text{mol}^{-1}$ ) for  $C_4H_2$  and  $C_4D_2$

	$C_4H_2$	$C_4D_2$	Popov et al. <sup>a</sup>
$\Sigma_u^+$	$1.21 \pm 0.05$	$1.21 \pm 0.05$	$0.61 \pm 0.03$
$\Pi_u$	$55 \pm 3$	$51 \pm 4$	—

<sup>a</sup>Ref 2

## DIPOLE MOMENT DERIVATIVES

In the harmonic oscillator—linear dipole moment approximation the relation between the absolute intensity  $A_i$  of the  $i$ th fundamental absorption band and the dipole moment derivative with respect to the normal coordinate  $Q_i$  becomes

$$A_i = \frac{N_0 \Pi g_i}{3c^2} \frac{\nu_i}{\omega_i} \left( \frac{\partial \vec{\mu}}{\partial Q_i} \right)^2 \quad (1)$$

Where  $N_0$  denotes Avogadro's number,  $g_i$  the degeneracy of the  $i$ th fundamental,  $\nu_i$  and  $\omega_i$  the experimental- and harmonic frequencies, respectively,  $c$  the velocity of light,  $\vec{\mu}$  the molecular dipole moment and  $Q_i$  the normal coordinate.

The dmd's given in Table 10 are obtained from  $P_S = P_Q L^{-1}$  where the elements of the  $P_S$  polar tensor are the dmd's, while  $P_Q$  contains the dipole moment derivatives with respect to normal coordinates. The  $L^{-1}$  matrix is defined by the transformation of symmetry coordinates to normal coordinates,  $Q = L^{-1} S$ .

The sign indeterminacy of the  $\partial \vec{\mu} / \partial Q_i$  quantities obtained from eqn. (1) yields 16 different  $\partial \vec{\mu} / \partial Q$  sign combinations, in principle leading to 16 different  $P_S$  polar tensors. However, taking into account the molecular symmetry and the fact that only the relative signs of the dmd's within a symmetry block can be determined, the latter number reduces to 4. From the 8 experimental intensity values of Table 8, two sets of dmd's could be calculated by use of the non-linear least-squares fitting procedure used earlier [16, 18]. The starting values were obtained from the experimental  $C_4H_2$  intensities using the four possible sign combinations for the  $\partial \vec{\mu} / \partial Q_i$  parameters. The starting values were adjusted to fit the experimental intensities. The four

TABLE 10

Dmd values ( $DA^{-1}$ ) for diacetylene, propyne and acetylene<sup>a</sup>

	Diacetylene		Propyne <sup>b</sup>	Acetylene <sup>c</sup>
	Set 1 <sup>d</sup>	Set 2 <sup>d</sup>		
$\partial \vec{\mu}_z / \partial S_A$	$1.621 \pm 0.027$	$1.621 \pm 0.064$	$1.232 \pm 0.028$	$1.264 \pm 0.016$
$\partial \vec{\mu}_z / \partial S_i$	$-1.062 \pm 0.018$	$-1.062 \pm 0.042$	$-1.737 \pm 0.06$	
$\partial \vec{\mu}_x / \partial S_{xx}$	$1.482 \pm 0.035$	$1.089 \pm 0.088$	$1.519 \pm 0.06$	$1.482 \pm 0.022$
$\partial \vec{\mu}_x / \partial S_{xx}$	$1.294 \pm 0.028$	$-0.614 \pm 0.069$	$1.141 \pm 0.028$	
Res.	5.78	33.51		

<sup>a</sup>The stated errors are standard deviations resulting from the least-squares fitting procedure. <sup>b</sup>Ref. 18; dmd value multiplied by  $2^{1/2}$  to allow direct comparison. E-type dmd's with respect to a  $C_4$ ,  $C_2$  reference coordinate. <sup>c</sup>Ref. 19. <sup>d</sup>The signs for the corresponding  $\partial \vec{\mu} / \partial Q_i$  parameters are in case of set 1:  $+-$ ,  $++$  for  $C_4H_2$  and  $+-$ ,  $++$  for  $C_4D_2$ , whereas set 2 corresponds to:  $+-$ ,  $+-$  for  $C_4H_2$  and to  $++$ ,  $+-$  for  $C_4D_2$ .

starting sets converged to the two final sets given in Table 10 and for comparison, the corresponding values for propyne [18] and acetylene [19] are also given. For each set the residual resulting from the least-squares fitting procedure is also shown in this Table. The residuals are defined as

$$\text{Res} = \sum_i \{A_i(\text{exp}) - A_i(\text{calc})\}^2 / \text{Err}_i^2 \quad (2)$$

where  $A_i(\text{exp})$  denotes the experimental intensity given in Table 8,  $A_i(\text{calc})$  is the corresponding calculated intensity,  $\text{Err}_i$  is the stated standard deviation and the summation extends over all intensity data. In view of the disagreement between the signs for  $\partial \bar{\mu}_x / \partial S_{9x}$  of diacetylene and propyne in the case of set 2 on one hand and its larger residual on the other this set must be rejected. The signs of the dmd's of set 1 are in full agreement with propyne and acetylene.

Nevertheless, the values for the  $\Sigma$ -type dmd's show substantial differences. The  $\partial \bar{\mu}_z / \partial S_4$  value of diacetylene is much larger than the corresponding value for propyne and acetylene. A similar discrepancy was observed for the dmd's pertaining to the symmetrical methyl stretching modes of propyne and butyne-2 [16]. We shall return to this point in the next section. Further, the dmd value for the hydrogen bending mode of diacetylene ( $\partial \bar{\mu}_x / \partial S_{8x}$ ) is in complete agreement with the values for propyne [18] and acetylene [19], indicating that the  $\equiv\text{C}-\text{H}$  bond is quite insensitive to changes in the neighbouring bond. In order to allow comparison of the dmd's belonging to the skeletal bending modes ( $\partial \bar{\mu}_x / \partial S_{9x}$ ) the propyne dmd is given with respect to a  $\text{C}_4$ ,  $\text{C}_5$  reference coordinate (see ref. 18). Neglecting any possible systematic errors in the  $\nu_9$  intensities the difference between the diacetylene and propyne value reflects the difference in the  $\text{C}\equiv\text{C}$  bond moments (see next section).

The absolute intensities for  $\text{C}_4\text{H}_2$  and  $\text{C}_4\text{D}_2$  calculated from the final set dmd's are given in Table 11. Comparison with the experimental intensities given in Table 8 shows that all differences between experimental and calculated

TABLE 11

Predicted intensities for  $\text{C}_4\text{H}_2$  and  $\text{C}_4\text{D}_2$  calculated from the final set dmd values<sup>a</sup> (Units are  $\text{km mol}^{-1}$ )

$A_i$	$\text{C}_4\text{H}_2$ <sup>b</sup>	$\text{C}_4\text{D}_2$ <sup>b</sup>
$A_4$	$131 \pm 3$	$81.0 \pm 1.6$
$A_5$	$1.90 \pm 0.10$	$0.46 \pm 0.06$
$A_6$	$160 \pm 6$	$84 \pm 4$
$A_8$	$6.20 \pm 0.29$	$7.70 \pm 0.28$

<sup>a</sup>See set 1 of Table 10 for final dmd values <sup>b</sup>The values for the dispersions only contain the errors propagated from the dispersions in the dmd's of Table 10 set 1.

values are within the stated error limits. In Table 12 the predicted fundamental frequencies and absolute intensities of  $C_4HD$  are shown.

The predicted harmonic frequencies were calculated using the final force field of Table 6, whereas the anharmonic frequencies were obtained by using the anharmonicity constants of  $C_4H_2$  adjusted according to Dennison's rule [9].

Since the  $C_4HD$  intensities predicted with the final dmd's compare very well with those based on the experimental  $C_4H_2$  intensities alone, as can be seen from Table 12, the correction of the  $C_4D_2$  intensities for the  $C_4HD$  impurity needs no adjustment.

#### BOND CHARGE PARAMETERS

The dipole moment derivatives can be further reduced to bcp's. These parameters are based on a simple point charge model of the valence electrons [20] and consist of bond charges and bond charge derivatives. The bond charges,  $q_k$ , are defined by

$$\vec{\mu} = \sum_k \sum_{\sigma} \vec{\mu}_{k\sigma} = \sum_k \sum_{\sigma} q_k r_k \vec{e}_{k\sigma} \quad (\sigma = x, y \text{ or } z) \quad (3)$$

where  $\vec{\mu}_k$  is the bond moment of the  $k$ -th bond,  $q_k$  being the bond charge,  $r_k$  the bond length and  $\vec{e}_{k\sigma}$  the  $\sigma$  component of the bond unit vector. The bond charge derivatives,  $\partial q_k / \partial R_j$ , appear by substitution of eqn. (3) into the  $\partial \vec{\mu} / \partial R_j$  quantities, giving

$$\partial \vec{\mu} / \partial R_j = \sum_k \sum_{\sigma} \{ r_k \vec{e}_{k\sigma} (\partial q_k / \partial R_j) + q_k \vec{e}_{k\sigma} (\partial r_k / \partial R_j) + q_k r_k (\partial \vec{e}_{k\sigma} / \partial R_j) \} \quad (4)$$

TABLE 12

Predicted fundamental frequencies ( $\text{cm}^{-1}$ ) and absolute intensities ( $\text{km mol}^{-1}$ ) for  $C_4HD$

	$\nu_i$	$\omega_i$	$A_i^a$	$A_i^b$
$\nu_1$ (C—H str.)	3334	3492	$65.6 \pm 1.5$	$67.8 \pm 2.7$
$\nu_2$ (C≡C sym. str.)	2146	2178	$1.97 \pm 0.04$	$1.98 \pm 0.05$
$\nu_3$ (C—C str.)	860	873	$0.0070 \pm 0.0002$	$0.0070 \pm 0.0004$
$\nu_4$ (C—D str.)	2601	2695	$39.8 \pm 0.8$	$41.0 \pm 1.6$
$\nu_5$ (C≡C asym. str.)	1937	1965	$0.002 \pm 0.003$	$0.009 \pm 0.012$
$\nu_6$ (C—H bend)	629	644	$84 \pm 3$	$91 \pm 7$
$\nu_7$ (C≡C—C asym. bend)	466	473	$10.3 \pm 0.5$	$11.1 \pm 0.9$
$\nu_8$ (C—D bend)	503	512	$27.9 \pm 1.2$	$29.8 \pm 2.4$
$\nu_9$ (C≡C—C sym. bend)	211	214	$7.07 \pm 0.28$	$7.1 \pm 0.4$

<sup>a</sup>Predicted from the final dmd values (set 1 of Table 10). The standard deviations only contain the errors propagated from the corresponding dispersions in the dmd's. <sup>b</sup>Based on the experimental  $C_4H_2$  data only.

The direction of  $\vec{e}_k$  corresponds to the direction of  $\vec{\mu}_k$ , which points from the negatively to the positively charged end of the bond. This choice for the direction of the bond unit vector immediately implies that the bond charges  $q_k$  are positive numbers, as may be seen from the last part of eqn. (3). From the expressions of the symmetry coordinates in terms of internal coordinates (see Table 7) the following relations may be easily verified

$$\begin{aligned}\partial\vec{\mu}_z/\partial S_4 &= 2^{1/2}\partial\vec{\mu}/\partial r_1 \\ \partial\vec{\mu}_z/\partial S_5 &= 2^{1/2}\partial\vec{\mu}/\partial r_2 \\ \partial\vec{\mu}_x/\partial S_{8x} &= 2^{1/2}\partial\vec{\mu}_x/\partial\phi_{1x} \\ \partial\vec{\mu}_x/\partial S_{9x} &= 2^{1/2}\partial\vec{\mu}_x/\partial\beta_{1x}\end{aligned}\quad (5)$$

Making use of eqns. (3), (4) and (5) and the bond moment directions defined in Fig. 1, the dmd's can be expressed in terms of bcp's, as given in Table 13.

In view of the positive value obtained for  $\partial\vec{\mu}_x/\partial S_{8x}$  and its expression in terms of  $q_1$  the C-H moment of diacetylene must coincide with the corresponding directions found in propyne [18] and acetylene [19]. Furthermore, since the value of  $\partial\vec{\mu}_x/\partial S_{9x}$  is smaller than the value of  $\partial\vec{\mu}_x/\partial S_{8x}$  (see Table 10) it is easily seen from the last two expressions of Table 13 that  $\vec{\mu}_1$  and  $\vec{\mu}_2$  must have opposite directions. The direction of the zero C-C bond moment may be chosen arbitrarily.

The expressions of the dmd's in terms of bcp's may be solved for the bond charges  $q_1$ ,  $q_2$  and the charge flux terms  $r_1(\partial q_1/\partial r_1) - r_2(\partial q_2/\partial r_1) - r_3(\partial q_3/\partial r_1) + r_4(\partial q_4/\partial r_1) - r_5(\partial q_5/\partial r_1)$  and  $r_1(\partial q_1/\partial r_2) - r_2(\partial q_2/\partial r_2) - r_3(\partial q_3/\partial r_2) - r_4(\partial q_4/\partial r_2) - r_5(\partial q_5/\partial r_2)$ . Values for the bond charges and charge fluxes obtained from the final dmd's of Table 10, are given in Table 14.

In a previous paper [1] we presented common sets of bcp's for  $C_2H_2$ ,  $CH_3C\equiv CH$  and  $CH_3C\equiv CCH_3$ . For comparison, the values of the common bcp's which correspond to those of diacetylene for three different common sets are given in Table 14. Also, the corresponding values of the common set proposed by Jona et al. [21], are given in this Table.

It appears from Table 14 that the  $q_1$  bond charge is in nice agreement with the corresponding values found for propyne and acetylene showing, as mentioned above, the invariance of  $q_1$  on substitution at the other side of the triple bond. The rather small value found for  $q_2$  as compared to the common

TABLE 13

Dipole moment derivatives of diacetylene expressed in bond-charge parameters

$\partial\vec{\mu}_z/\partial S_4$	$= 2^{1/2}\{r_1(\partial q_1/\partial r_1) - r_2(\partial q_2/\partial r_1) - r_3(\partial q_3/\partial r_1) + r_4(\partial q_4/\partial r_1) - r_5(\partial q_5/\partial r_1) + q_1\}\vec{e}_z$
$\partial\vec{\mu}_z/\partial S_5$	$= 2^{1/2}\{r_1(\partial q_1/\partial r_2) - r_2(\partial q_2/\partial r_2) - r_3(\partial q_3/\partial r_2) + r_4(\partial q_4/\partial r_2) - r_5(\partial q_5/\partial r_2) - q_2\}\vec{e}_z$
$\partial\vec{\mu}_x/\partial S_{8x}$	$= 2^{1/2}q_1r_1\vec{e}_x$
$\partial\vec{\mu}_x/\partial S_{9x}$	$= 2^{1/2}\{q_1r_1 - q_2r_2\}\vec{e}_x$

TABLE 14

Bond charge parameters for diacetylene and corresponding common values for propyne, acetylene and butyne-2<sup>a</sup>

Parameter	Diacetylene	Ref. 1 <sup>b</sup>	Ref. 1 <sup>c</sup>	Ref. 1 <sup>d</sup>	Jona et al. <sup>e</sup>
$q_1$	0.960	0.991	0.987	1.002	1.002
$q_2$	0.110	0.275	0.224	0.206	0.206
$\partial q_i/\partial r_1$	0.170 <sup>f</sup>	-0.098 <sup>g</sup>	-0.101 <sup>g</sup>	-0.109 <sup>g</sup>	-0.104 <sup>g</sup>
$\partial q_i/\partial r_2$	0.526 <sup>h</sup>	0.800 <sup>i</sup>	0.862 <sup>i</sup>	0.855 <sup>i</sup>	0.745 <sup>i</sup>

<sup>a</sup>Units:  $q$  in DA<sup>-1</sup> and  $\partial q/\partial r$  in DA<sup>-2</sup>. <sup>b</sup>Table 7. <sup>c</sup>Table 10 column 1. <sup>d</sup>Table 10 column 11.

<sup>e</sup>Ref. 21.

$$^f \partial q_i/\partial r_1 = (\partial q_1/\partial r_1) - (r_2/r_1)(\partial q_2/\partial r_1) - (r_3/r_1)(\partial q_3/\partial r_1) + (r_4/r_1)(\partial q_4/\partial r_1) - (r_5/r_1)(\partial q_5/\partial r_1).$$

$$^g \partial q_i/\partial r_1 = (\partial q_1/\partial r_1) - (r_2/r_1)(\partial q_2/\partial r_1)$$

$$^h \partial q_i/\partial r_2 = (\partial q_2/\partial r_2) + (r_3/r_2)(\partial q_3/\partial r_2) - (r_1/r_2)(\partial q_1/\partial r_2) - (r_4/r_2)(\partial q_4/\partial r_2) + (r_5/r_2)(\partial q_5/\partial r_2)$$

$$^i \partial q_i/\partial r_2 = (\partial q_2/\partial r_2) + (r_3/r_2)(\partial q_3/\partial r_2) - (r_1/r_2)(\partial q_1/\partial r_2).$$

set values reflects the difference between conjugated and isolated triple bonds. Clearly, the polarity of the C≡C bond decreases by conjugation. The value of the charge flux parameters differ considerably from those predicted by the common sets. This may be due to the difference in equilibrium charge distribution due to  $\pi$  electron delocalization in diacetylene or to the fact that long-range bcp's may have unusually large values in symmetrical molecules such as diacetylene. In the calculation of the common sets [1] the only non-zero charge derivatives were  $\partial q_i/\partial r_i$  and  $\partial q_i/\partial r_{i \pm 1}$ , while all derivatives with respect to remote coordinates ( $\partial q_i/\partial r_j = 0, |i - j| > 1$ ) were assumed to be zero. In the discussion of the results in ref. 1 we mentioned the possibility that in a symmetrical molecule like butyne-2 the assumption of zero long-range bcp's may not be valid. The in-phase motions of identical bonds (e.g.,  $S_4$  and  $S_5$  in diacetylene) may lead to enhanced charge fluxes for distortions along remote coordinates. The above discussion reveals that bcp's (and similar local polar parameters such as eop's) are only transferable between similar bonds in similar environments. This means that the dmd's of a rather large number of basic molecules must be obtained before successful common sets can be derived. From the bond moments of diacetylene we can easily obtain a set of corresponding atomic charges as given in the first column of Table 15. For comparison the net atomic charges derived from ab initio studies [22, 23] are given. The charges of H and C<sub>2</sub> are in poor agreement with the ab initio values. The charges given by Moffat [22] are much lower than the experimental values whereas those of Powell et al. [23] are much higher. This once again demonstrates the impossibility of defining uniquely physical quantities which are not unequivocally connected to an observable. Both the experimental and ab initio values are based upon a rather arbitrarily chosen model which hampers direct comparison of the calculated values. Clearly, no



TABLE 15

Atomic charges (e) for diacetylene

	This work	Ref. 22	Ref. 23
$q_H$	0.200	0.117	0.362
$q_{C_1}$	-0.246	-0.385	-0.333
$q_{C_3}$	0.023	-0.030	-0.052

conclusions can be drawn from the small values for the charge on  $C_3$ , the opposite signs may very well be caused by the different models underlying these values. Useful comparisons between experimental and theoretical "atomic charges" would become possible if a quantum-mechanical atomic charge definition could be found, leading to charges in agreement with quantum mechanically calculated dmd values. Obviously, the availability of such an "atomic charge" definition would be very useful for the interpretation of intensity studies.

From this study it may be concluded that the bcp's of an isolated ethynyl group are quite different from those of conjugated systems. Only the C—H bond charge seems hardly to be affected by conjugation of the ethynyl group. This again emphasizes that an acceptable transferability of bcp's may only be expected for very similar molecules.

## REFERENCES

- 1 Th. Koope and W. M. A. Smit, *J. Mol. Struct.*, **113** (1984) 25.
- 2 E. M. Pappov, I. P. Palovnev, E. D. Lubuzht and G. A. Kogan, *Zh. Fizik. Spektrosk.*, **8** (1968) 463.
- 3 L. Brandsma and H. D. Verkruijsse, *Synthesis of Acetylenes, Allenes and Cumulenes*, Elsevier, Amsterdam, 1981, p. 146.
- 4 A. V. Jones, *Proc. R. Soc., Ser. A*, **211** (1952) 285.
- 5 I. Freund and R. S. Hallgren, *J. Chem. Phys.*, **42** (1965) 4131.
- 6 J. L. Hardwick, D. A. Ramsay, J. M. Garneau, J. Lavigne and A. Cabana, *J. Mol. Spectrosc.*, **76** (1979) 492.
- 7 F. Windler, *Z. Naturforsch.*, Teil A, **28** (1973) 1179.
- 8 J. L. Duncan, D. C. McKean and G. D. Nivellini, *J. Mol. Struct.*, **32** (1976) 255.
- 9 D. M. Dennison, *Rev. Mod. Phys.*, **12** (1940) 175.
- 10 E. B. Wilson Jr., J. C. Decius and P. C. Cross, *Molecular Vibrations*, McGraw-Hill, New York, 1955, Chap. 8.
- 11 M. Tanimoto, K. Kuchitsu and Y. Morino, *Bull. Chem. Soc. Jpn.*, **44** (1971) 385.
- 12 P. A. Sipos and M. K. Phibbs, *Can. J. Spectrosc.*, **19** (1974) 159.
- 13 E. B. Wilson Jr. and A. J. Wells, *J. Chem. Phys.*, **14** (1946) 578.
- 14 S. S. Penner and D. T. Weber, *J. Chem. Phys.*, **19** (1951) 307.
- 15 A. G. Worthing and J. Geffner, *Treatment of Experimental Data*, Wiley, New York, 1947, Chap. 11.
- 16 Th. Koope, T. Visser, W. M. A. Smit, L. Brandsma and H. D. Verkruijsse, *J. Mol. Struct.*, **100** (1983) 95.
- 17 (a) B. L. Crawford Jr., *J. Chem. Phys.*, **20** (1952) 977. (b) W. M. A. Smit, *J. Chem. Phys.*, **70** (1979) 5336.

- 18 J. H. G. Bode, W. M. A. Smit, T. Visser and H. D. Verkruijsse, *J. Chem. Phys.*, **72** (1980) 6560.
- 19 Th. Koops, W. M. A. Smit and T. Visser, *J. Mol. Struct.*, **112** (1984) 285.
- 20 A. J. van Straten and W. M. A. Smit, *J. Mol. Spectrosc.*, **62** (1976) 297; **65** (1977) 202.
- 21 P. Jona, M. Gussoni and G. Zerbi, *J. Phys. Chem.*, **85** (1981) 2210.
- 22 J. B. Moffat, *J. Mol. Struct.*, **42** (1977) 251.
- 23 M. F. Powell, M. R. Peterson and I. G. Csizmadia, *J. Mol. Struct., Theochem*, **92** (1983) 323.